Supporting Information

Ultra Elastic, Stretchable, Self-Healing Conductive Hydrogels with Tunable Optical properties for Highly Sensitive Soft Electronic Sensors

Meng Wu[1], Jingsi Chen[1], Yuhao Ma[2], Bin Yan[3], Mingfei Pan[1], Qiongyao Peng[1], Wenda Wang[1], Linbo Han[4], Jifang Liu[5], Hongbo Zeng[1,]*

[1] *Department of Chemical and Materials Engineering, University of Alberta, Edmonton, Alberta T6G 1H9, Canada*

[2] *Department of Biomedical Engineering, University of Alberta, Edmonton, Alberta T6G 2V2, Canada*

[3]*College of Biomass Science and Engineering, Sichuan University, Chengdu, Sichuan, China*

[4]*College of Health Science and Environmental Engineering, Shenzhen Technology University, Shenzhen 518118, China*

[5] *The Fifth Affiliated Hospital, Guangzhou Medical University, Guangzhou, Guangdong, 510700, China*

**Corresponding Author. E-mail: hongbo.zeng@ualberta.ca (H. Zeng), Phone: +1-780-492-1044*

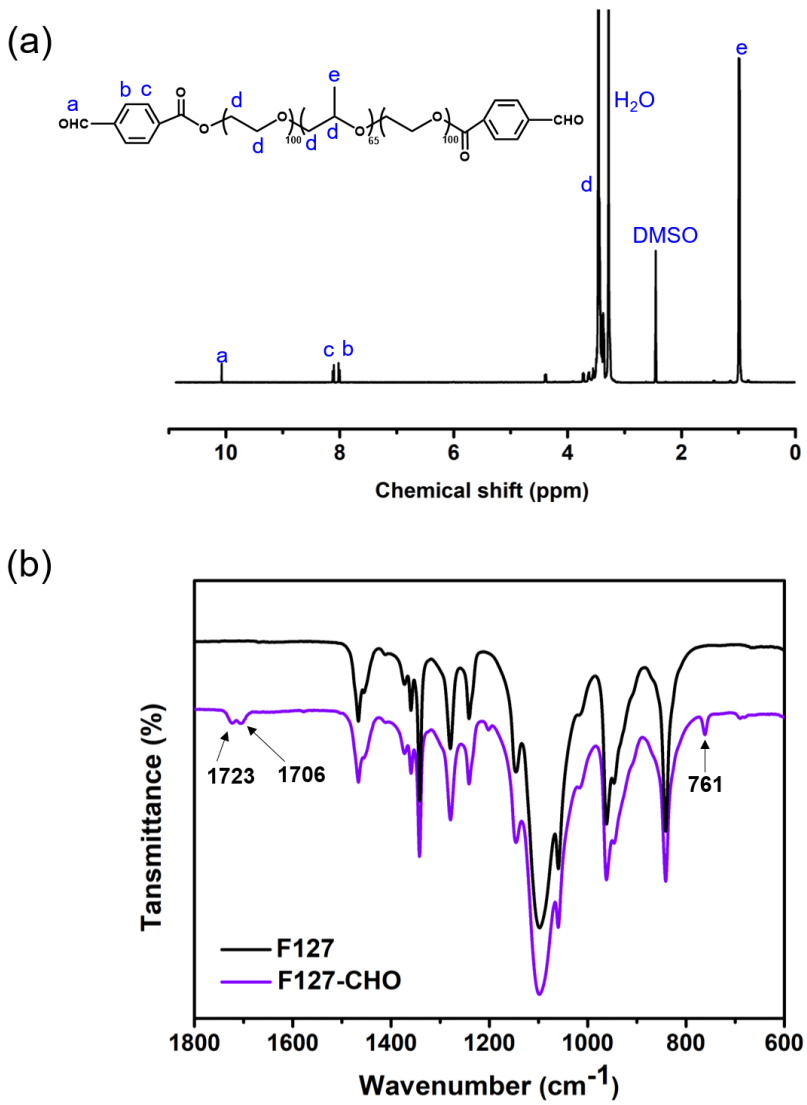

Figure S1. (a) ^{1}H NMR and (b) FTIR spectra of F127-CHO.

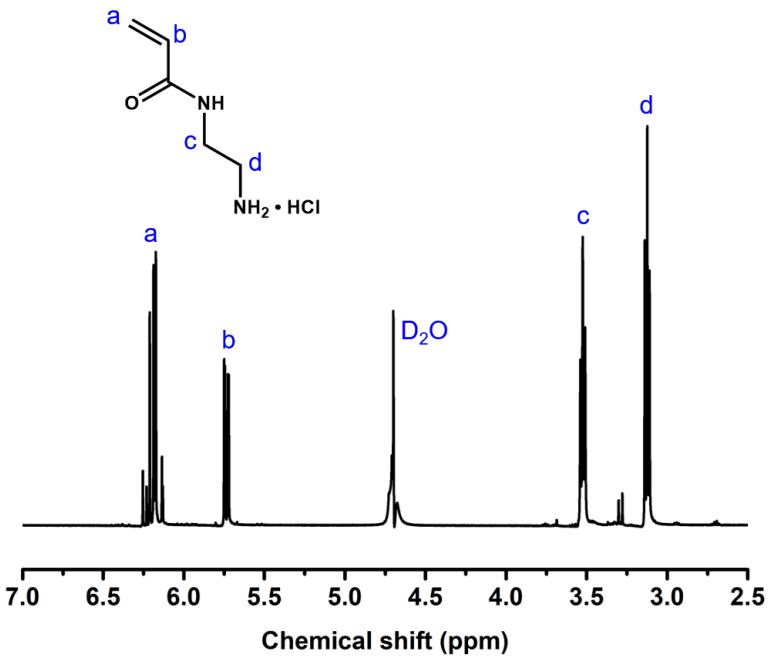

Figure S2. ^{1}H NMR spectrum of 2-aminoethyl acrylamide hydrochloride (AEAM).

Table S1. Water contents of hydrogels with different compositions.

Sample	Water content (%)
PAM	75.7
PAMF	78.8
PAAF	75.8
PAAFC	75.6
PAAFC-L	73.9

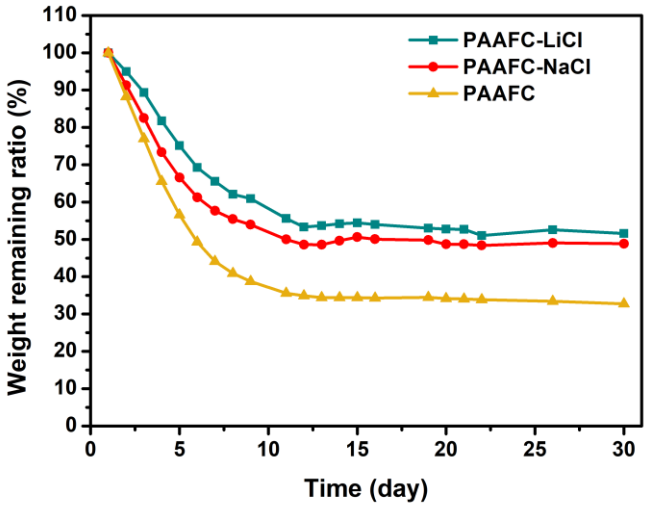

Figure S3. Weight change of PAAFC hydrogel with LiCl, NaCl and without addition of ions under ambient condition (70−80 RH%, 20 °C).

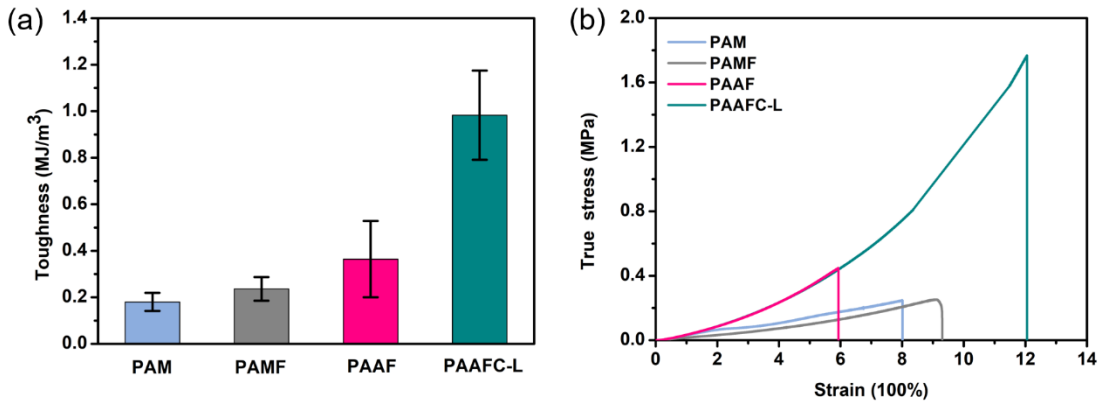

Figure S4. (a) Toughness and (b) true stress of hydrogels with different compositions.

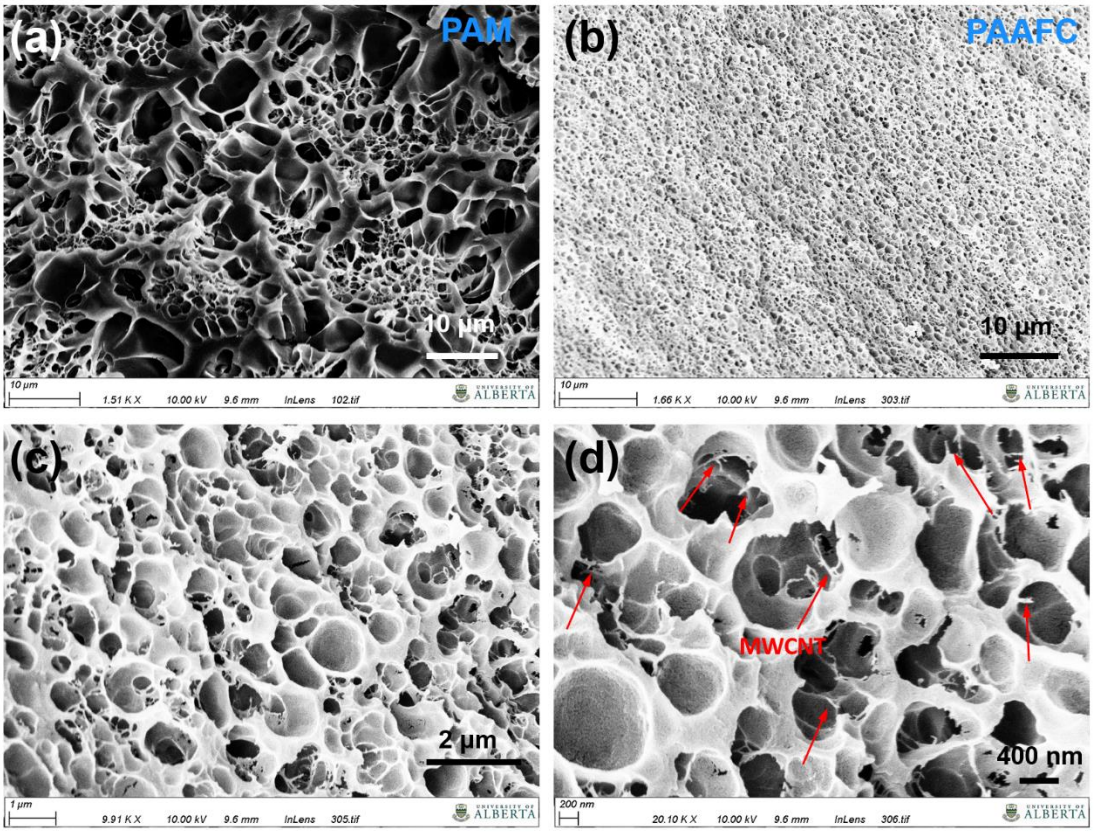

Figure S5. SEM images of the cross-sections of freeze-dried (a) PAM hydrogel, (b) PAAFC hydrogel, (c) and (d) PAAFC at higher magnifications. Red arrows indicating the MWCNTs.

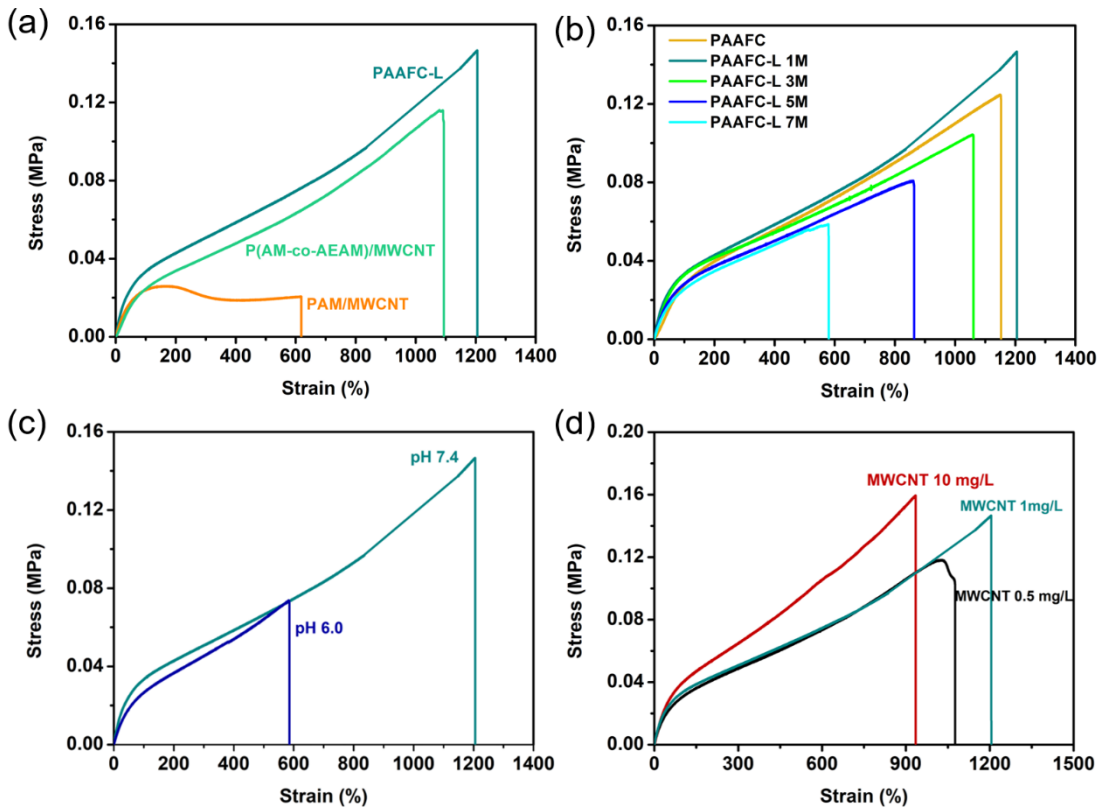

Figure S6. Stress-strain curves of (a) PAAFC-L, PAM/MWCNT and P(AM-co-AEMA)/MWCNT hydrogels, (b) hydrogels with different concentrations of LiCl, (c) PAAFC-L hydrogels prepared at different pH, and (d) PAAFC-L hydrogels with various MWCNT concentrations.

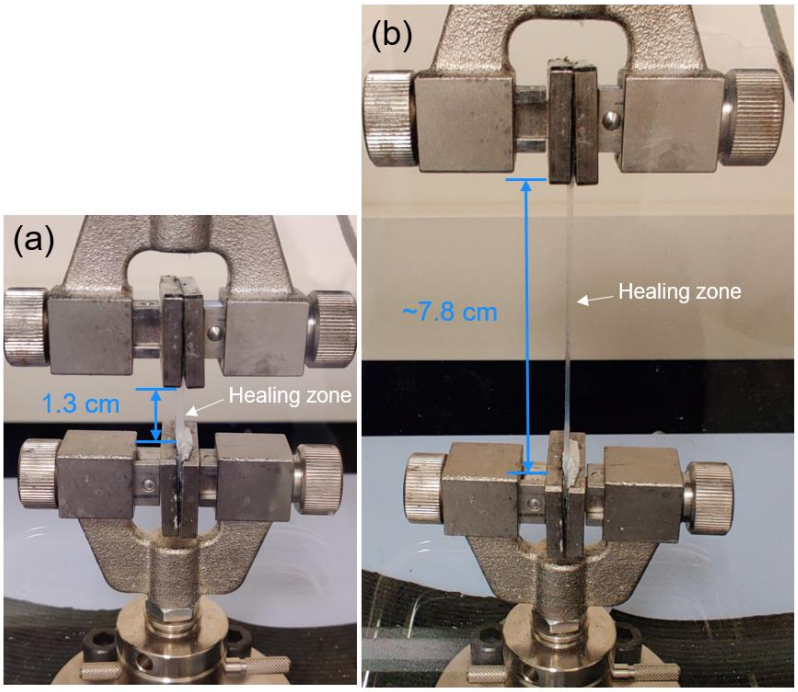

Figure S7. Photographs showing the PAAFC-L hydrogel self-healing for 24 h (a) before and (b) during stretching.

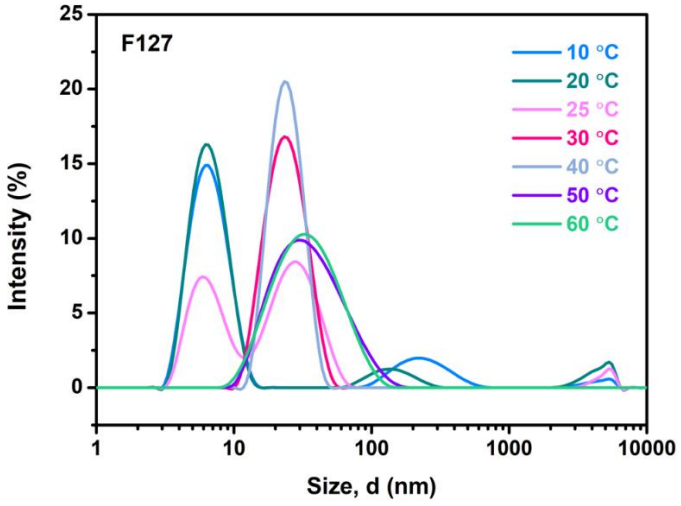

Figure S8. DLS size characterization results of unmodified F127 micelles at various temperatures ranging from 10 to 60 °C.

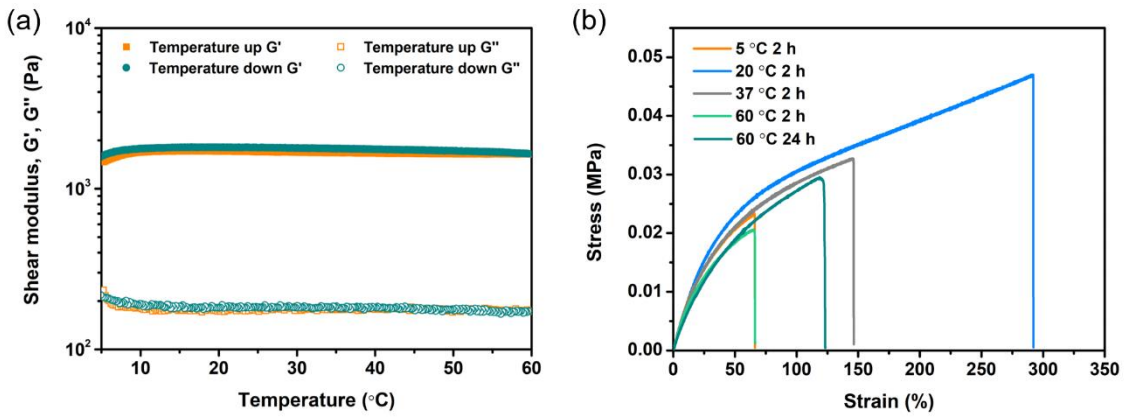

Figure S9. (a) Rheological oscillatory temperature sweeps of PAAFC-L hydrogel at an angular frequency of 10 rad/s and a strain of 1%. (b) Stress-strains curves of PAAFC-L hydrogels healed at different temperatures.

As shown in Figure S9b, the hydrogel healed at room temperature displayed the best anti-stretching performance. Both lowering and raising temperature would impair the stretchability of self-healed PAAFC-L hydrogel. It is known the self-healing property of a hydrogel relies on several factors, where the most important ones are the dynamic nature of the cross-linking bonds and the mobility of polymer chains within the hydrogel. At 5 °C, the low chain mobility and increased hydrophobic associations in PAAFC-L hydrogel hinder the self-healing of the hydrogel. Considering the molecular mobility should be enhanced at higher temperatures (37 and 60 °C), the decreased self-repairing efficiency with the increasing of temperature above room temperature is most likely caused by the reduction of dynamicity of the cross-linking bonds. Among the dynamic bonds involved for PAAFC-L hydrogel construction, imine bonds play an important role in self-healing of the hydrogel. The dynamic nature of imine bond originates from the reversible imine formation reaction, i.e., imine hydrolysis and re-formation reach a thermodynamic equilibration under experimental conditions, and imine exchange reactions.[1,2] Although raising temperature is favorable for exchange reactions, imine formation is also facilitated at the same time.[3] That is, at elevated temperatures, the equilibrium of Schiff base reaction is pulled toward imine formation and the hydrolysis process would be suppressed, which might lead to reduced reversibility of the bond and the impaired self-healing behavior.

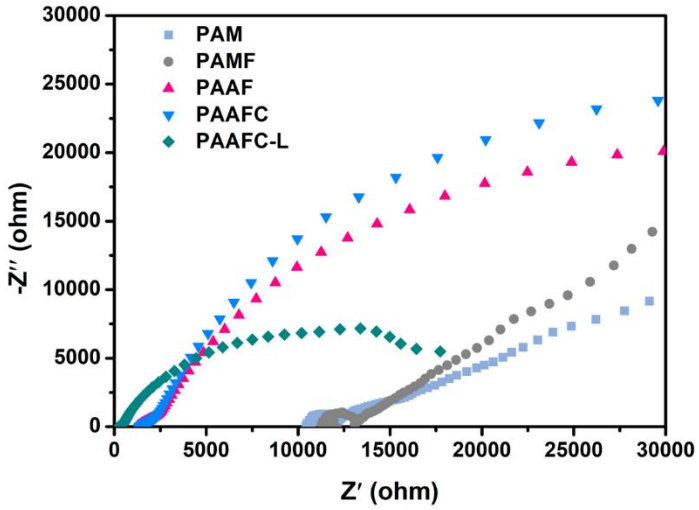

Figure S10. Electrochemical impedance spectra of hydrogels of various compositions.

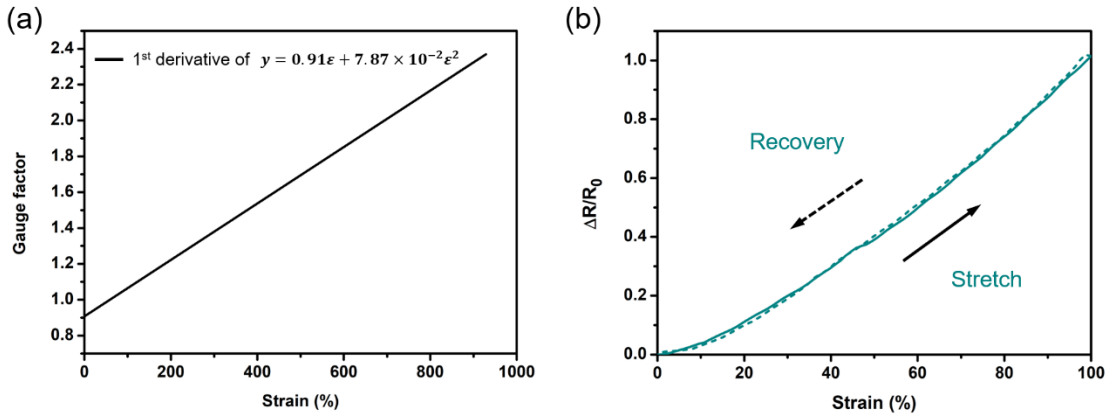

Figure S11. (a) Plot of gauge factor versus strain for PAAFC-L hydrogel calculated from the differentiation of the fitting curve of relative resistance change versus strain experimental data. (b) Relative resistance change-tensile strain loading-unloading curves of PAAFC-L hydrogel. Dash line indicating the recovery process.

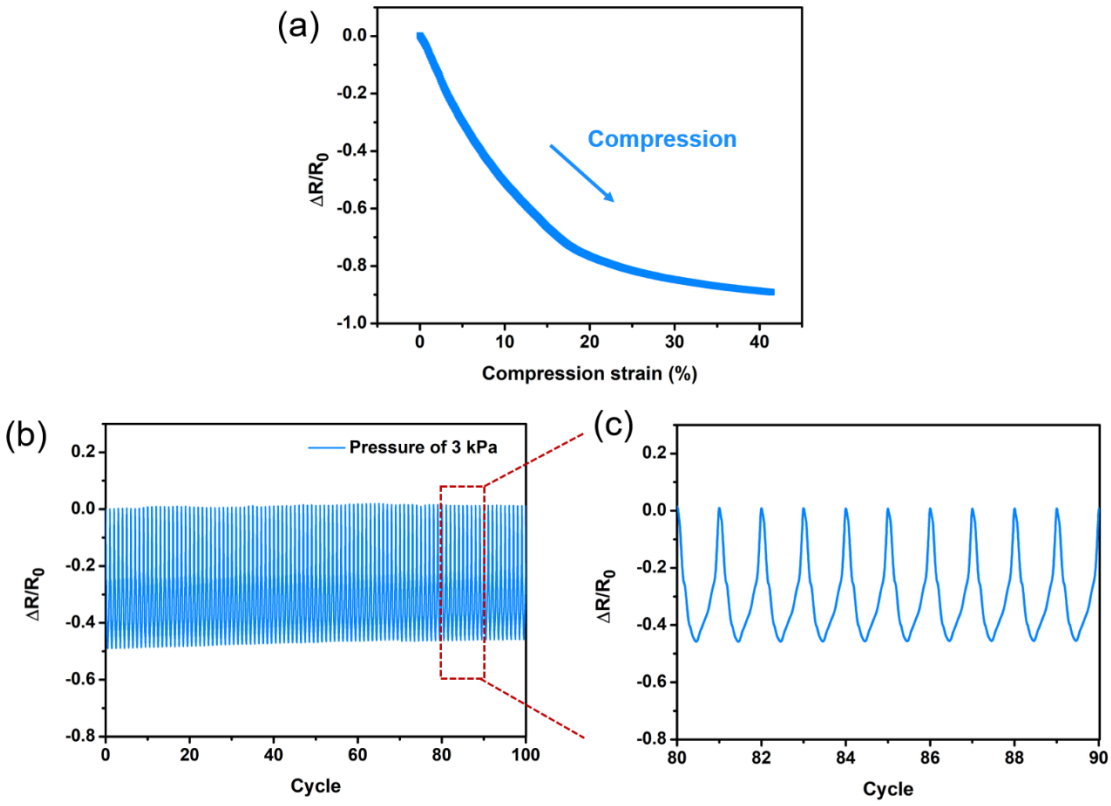

Figure S12. (a) Relative resistance variation as a function of compression strain for PAAFC-L hydrogel. (b) Relative resistance response of the PAAFC-L hydrogel under cyclic pressure loading of 3 kPa (compression strain of 10%) for 100 cycles. (c) Magnified signal during 80-90 cycles.

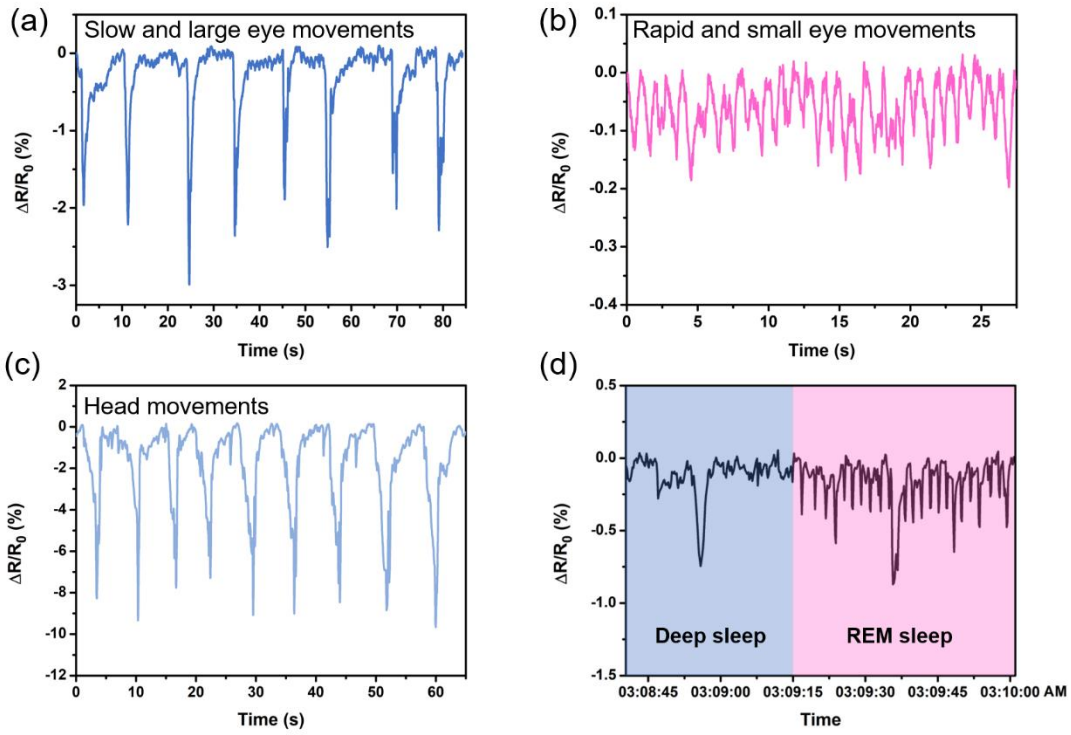

Figure S13. Relative resistance changes of (a) slow and large eye movements, (b) rapid and small eye movements, and (c) head movements measured under awake state. (d) Relative resistance change curve showing the transition from deep to REM sleep.

Table S2. Comparison of reported elastic hydrogels with this work

Components of hydrogels	Stretchability	Stress at break (MPa)	Elasticity[a]		Self-healing efficiency[b]	Stretchability after self-healing	Stimuli-responsiveness	Conductivity (S/m)	Ref.
			Stretching	Compression					
P(AM-co-AEAM) /MWCNT /F127-CHO/LiCl	1205%	0.147	97% Strength recovery for 1000% strain at 20th cycle	Complete recovery for 90% strain	53%	636%	Thermo-responsive	3.96	**This work**
Sodium alginate /NaCl/PAM	3120%	0.75	98% Energy dissipation recovery for 1000% strain at 20th cycle	Complete recovery for 98% strain	n/a	n/a	n/a	0.023	4
UPyHCBA/SDS /NaCl /PAM	>10000%	0.004	93% Energy dissipation recovery for 500% strain at 2nd cycle	n/a	100%	>10000%	n/a	n/a	5
Hydroxypropyl cellulose/PVA/NaCl	975%	1.3	n/a	Recovery after compression	n/a	n/a	n/a	3.4	6
GO/MeTro	~210%	~0.02	~60% Strength recovery for 100% strain at 1000th cycle	n/a	n/a	n/a	n/a	n/a	7
PVA/PVP/CNC/Fe^{3+}	830%	2.1	60% Energy dissipation recovery for 500% strain at 2nd cycle	n/a	n/a	~150%	n/a	n/a	8
PAM/AETA/sulfonate-modified silica nanoparticles	370%	0.006	97% Energy dissipation recovery for 100% strain at 100th cycle	n/a	n/a	n/a	n/a	2.9	9
Agar/PAM/Stearyl methacrylate (SMA)/SDS	5260%	0.267	40% of Energy dissipation recovery for 900% strain at 2nd cycle (2 min)	n/a	40%	170%	n/a	n/a	10
PAM/Alginate/Ca^{2+}	2200%	0.156	74% of Energy dissipation recovery for 600% strain at 2nd cycle (80 °C, 1 day)	n/a	n/a	n/a	n/a	n/a	11

PAM/F127 diacrylate	2300%	0.27	98% Shape recovery for 1000% strain at 2nd cycle (30 h)	Complete recovery for 90% strain	n/a	n/a	Thermo-responsive	n/a	12
PAAc/SMA/CTAB /NaBr	800−900%	0.7−1.7	97% Strength recovery for 500% strain (5 min)	Complete recovery for 92% strain	60−100% (treated at 35 °C with surfactant)	600−900%	Thermo-responsive	n/a	13
PAM/cucurbit[8]uril/ 1-benzyl-3-vinylimidazolium (host-guest)/MBAA	2400%	0.13	100% Strength recovery for 800% strain at 2nd cycle (2 min)	n/a	n/a	n/a	n/a	n/a	14
DMAA/MAAc	800%	1.3	100% of Energy dissipation recovery for 300% strain at 2nd cycle (60 min)	n/a	n/a	n/a	Thermo-responsive	n/a	15
SBMA/dopamine-modified clay/MBAA	900%	0.077	85% Strength recovery for 400% strain at 2nd cycle (3 min)	n/a	80%	859%	n/a	0.02	16
PMPTC/ PNaSS	750–800%	3.7	100% of Energy dissipation recovery for 300% strain at 2nd cycle (120 min)	n/a	66% (treated with NaCl)	630%	n/a	n/a	17
PAM/GO/Ca^{2+}	1100%	0.143	~90% Strength recovery for 700% strain	~90% recovery for 80% strain	n/a	n/a	n/a	n/a	18
PAM/CNT/SDS/ lauryl methacrylate	3000%	0.267	~90% Strength recovery for 1000% strain	Recovery from 70% strain	n/a	n/a	n/a	0.017	19
PAM/oxCNT/gelatin	1041%	0.71	Recovery from 500% strain	n/a	n/a	n/a	n/a	0.067	20

[a] The recovery percentages of the elasticity were obtained at room temperature with the wait time between cycles set within 1 min unless otherwise noticed.

[b] The self-healing efficiencies were obtained by tensile tests at room temperature without external stimuli unless otherwise noticed.

References

(1) Zhao, S.; Abu-Omar, M. M. Recyclable and Malleable Epoxy Thermoset Bearing Aromatic Imine Bonds. *Macromolecules* **2018**, 51, 9816-9824

(2) Chao, A.; Negulescu, I.; Zhang, D. Dynamic Covalent Polymer Networks Based on Degenerative Imine Bond Exchange: Tuning the Malleability and Self-Healing Properties by Solvent. *Macromolecules* **2016**, 49, 6277-6284

(3) Matsumoto, M.; Dasari, R. R.; Ji, W.; Feriante, C. H.; Parker, T. C.; Marder, S. R.; Dichtel, W. R. Rapid, Low Temperature Formation of Imine-Linked Covalent Organic Frameworks Catalyzed by Metal Triflates. *J. Am. Chem. Soc.* **2017**, 139, 4999-5002

(4) Zhang, X.; Sheng, N.; Wang, L.; Tan, Y.; Liu, C.; Xia, Y.; Nie, Z.; Sui, K. Supramolecular Nanofibrillar Hydrogels as Highly Stretchable, Elastic and Sensitive Ionic Sensors. *Materials Horizons* **2019**, 6, 326-333

(5) Jeon, I.; Cui, J.; Illeperuma, W. R. K.; Aizenberg, J.; Vlassak, J. J. Extremely Stretchable and Fast Self-Healing Hydrogels. *Adv Mater* **2016**, 28, 4678-4683

(6) Zhou, Y.; Wan, C.; Yang, Y.; Yang, H.; Wang, S.; Dai, Z.; Ji, K.; Jiang, H.; Chen, X.; Long, Y. Highly Stretchable, Elastic, and Ionic Conductive Hydrogel for Artificial Soft Electronics. *Adv Funct Mater* **2019**, 29, 1806220

(7) Annabi, N.; Shin, S. R.; Tamayol, A.; Miscuglio, M.; Bakooshli, M. A.; Assmann, A.; Mostafalu, P.; Sun, J. Y.; Mithieux, S.; Cheung, L. Highly Elastic and Conductive Human-Based Protein Hybrid Hydrogels. *Adv Mater* **2016**, 28, 40-49

(8) Liu, Y.-J.; Cao, W.-T.; Ma, M.-G.; Wan, P. Ultrasensitive Wearable Soft Strain Sensors of Conductive, Self-Healing, and Elastic Hydrogels with Synergistic "Soft and Hard" Hybrid Networks. *ACS applied materials & interfaces* **2017**, 9, 25559-25570

(9) Odent, J.; Wallin, T. J.; Pan, W.; Kruemplestaedter, K.; Shepherd, R. F.; Giannelis, E. P. Highly Elastic, Transparent, and Conductive 3d-Printed Ionic Composite Hydrogels. *Adv Funct Mater* **2017**, 27, 1701807

(10) Chen, Q.; Zhu, L.; Chen, H.; Yan, H.; Huang, L.; Yang, J.; Zheng, J. A Novel Design Strategy for Fully Physically Linked Double Network Hydrogels with Tough, Fatigue Resistant, and Self-Healing Properties. *Adv Funct Mater* **2015**, 25, 1598-1607

(11) Sun, J.-Y.; Zhao, X.; Illeperuma, W. R.; Chaudhuri, O.; Oh, K. H.; Mooney, D. J.; Vlassak, J. J.; Suo, Z. Highly Stretchable and Tough Hydrogels. *Nature* **2012**, 489, 133

(12) Sun, Y.-n.; Gao, G.-r.; Du, G.-l.; Cheng, Y.-j.; Fu, J. Super Tough, Ultrastretchable, and Thermoresponsive Hydrogels with Functionalized Triblock Copolymer Micelles as Macro-Cross-Linkers. *ACS Macro Letters* **2014**, 3, 496-500

(13) Gulyuz, U.; Okay, O. Self-Healing Poly (Acrylic Acid) Hydrogels with Shape Memory Behavior of High Mechanical Strength. *Macromolecules* **2014**, 47, 6889-6899

(14) Liu, J.; Tan, C. S. Y.; Yu, Z.; Lan, Y.; Abell, C.; Scherman, O. A. Biomimetic Supramolecular Polymer Networks Exhibiting Both Toughness and Self-Recovery. *Adv Mater* **2017**, 29, 1604951

(15) Hu, X.; Vatankhah-Varnoosfaderani, M.; Zhou, J.; Li, Q.; Sheiko, S. S. Weak Hydrogen Bonding Enables Hard, Strong, Tough, and Elastic Hydrogels. *Adv Mater* **2015**, 27, 6899-6905

(16) Pei, X.; Zhang, H.; Zhou, Y.; Zhou, L.; Fu, J. Stretchable, Self-Healing and Tissue-Adhesive Zwitterionic Hydrogels as Strain Sensors for Wireless Monitoring of Organ Motions. *Materials Horizons* **2020**, 7, 1872-1882

(17) Luo, F.; Sun, T. L.; Nakajima, T.; Kurokawa, T.; Zhao, Y.; Sato, K.; Ihsan, A. B.; Li, X.; Guo, H.; Gong, J. P. Oppositely Charged Polyelectrolytes Form Tough, Self-Healing, and Rebuildable Hydrogels. *Adv Mater* **2015**, 27, 2722-2727

(18) Cong, H.-P.; Wang, P.; Yu, S.-H. Highly Elastic and Superstretchable Graphene Oxide/Polyacrylamide Hydrogels. *Small* **2014**, 10, 448-453

(19) Qin, Z.; Sun, X.; Yu, Q.; Zhang, H.; Wu, X.; Yao, M.; Liu, W.; Yao, F.; Li, J. Carbon Nanotubes/Hydrophobically Associated Hydrogels as Ultrastretchable, Highly Sensitive, Stable Strain, and Pressure Sensors. *ACS Appl. Mater. Interfaces* **2020**, 12, 4944-4953

(20) Sun, X.; Qin, Z.; Ye, L.; Zhang, H.; Yu, Q.; Wu, X.; Li, J.; Yao, F. Carbon Nanotubes Reinforced Hydrogel as Flexible Strain Sensor with High Stretchability and Mechanically Toughness. *Chem Eng J* **2020**, 382, 122832